# Field Survey of the Camaná, Perú Tsunami of 23 June 2001

Emile A. Okal[1], Lori Dengler[2], Sebastian Araya[2], Jose C. Borrero[3], Brandon M. Gomer[1], Shun-ichi Koshimura[4,5], Gustavo Laos[6], Daniel Olcese[6], Modesto Ortiz F.[7], Matthew Swensson[3], Vasily V. Titov[4], and Fernando Vegas[6]*

## INTRODUCTION

On 23 June 2001 a major earthquake occurred at 20:33 UTC (3:33 PM local time) near the coast of southern Perú, 175 km west of Arequipa and 595 km southeast of Lima. The earthquake ruptured a portion of the plate boundary between the Pacific and Nazca Plates and produced ground shaking that was felt in much of southern Perú and northern Chile. It killed at least 57 people and destroyed or damaged more than 60,000 homes, affecting more than 223,000 people (USAID, 2001). The earthquake produced a tsunami that left an additional 24 people dead and 62 missing in the Camaná area (INDEC, 2001). This report summarizes the results of the first International Tsunami Survey Team (ITST) that surveyed the tsunami impacts two weeks after the earthquake and discusses the seismological characteristics of the earthquake that pertains to the tsunami.

## LOCATION, SIZE, AND FOCAL MECHANISM

The PDE location of the mainshock epicenter (USGS) is 16.26°S 73.64°W, about 60 km northwest of Ocoña in the Department of Arequipa, Perú; depth is unconstrained and fixed at 33 km. Figure 1A shows the epicenter and the extent of aftershocks over a 30-day window following the mainshock. The aftershock distribution suggests a 300-km-long by 125-km-wide rupture, extending southeast from the epicenter to the vicinity of Ilo, about 150 km north of the Chilean border.

Conventional magnitudes were $m_b$ 6.7 and $M_s$ 8.2; a mantle magnitude $M_m$ 8.6 (Okal and Talandier, 1989) was measured at Papeete (D. Reymond, pers. comm.), corresponding to a seismic moment $M_0 = 4 \times 10^{28}$ dyn-cm. Other estimates of the seismic moment, given in Figure 2, range from 1.2 to $4.9 \times 10^{28}$ dyn-cm. Harvard's final solution ($4.67 \times 10^{28}$ dyn-cm) gives the event the largest moment in the CMT catalog, making this the largest earthquake since the 1965 Rat Island, Alaska earthquake. Most focal solutions feature a thrust mechanism with a slight component of left-lateral strike-slip on a shallowly dipping fault plane striking 315° ± 10°, readily interpreted as representing the subduction of the Nazca Plate under South America. Only the "Quick" Harvard solution departs significantly from this geometry, trading off depth for the vertical dip-slip component of the moment tensor.

The dimension of the rupture can be estimated from the offset of Harvard's centroid location relative to the USGS epicenter, which is 150 km to the east-southeast. This agrees well with the aftershock distribution. In addition, Kikuchi and Yamanaka's (2001) tomographic slip distribution suggests a strong concentration of slip release around 16.9°S 72.2°W (Figure 1A). This point is only 60 km from the Harvard centroid, at the eastern end of a gap in the distribution of aftershocks, suggesting the rupture of a principal asperity, with a maximum slip of 4.5 m, at a location approximately 65 km east-southeast of Camaná.

## SLOWNESS AND DURATION OF SOURCE

A rather long source duration is documented both in the Harvard solution (86 s) and in Kikuchi and Yamanaka's (2001) model (107 s), the latter showing about a 40-second delay between the small hypocentral rupture and that of the main asperity. The slowness of the source was estimated using Newman and Okal's (1998) algorithm to compute an estimated-energy-to-moment ratio, which yielded a slowness parameter $\Theta = \log_{10} E/M_0 = -5.48 \pm 0.3$, on the basis of seven teleseismic stations. This number is intermediate between that predicted by universal scaling laws ($\Theta = -4.97$) and the deficient values ($\Theta < -6$) exhibited by the so-called "tsunami earthquakes" that are characterized by slow rupture possibly involving sedimentary material (Kanamori, 1972; Fukao, 1979; Polet and Kanamori, 2000). The intermediate slowness

1. Department of Geological Sciences, Northwestern University.
2. Department of Geology, Humboldt State University.
3. Department of Civil Engineering, University of Southern California.
4. Pacific Marine Environmental Laboratories, NOAA.
5. Present address: Disaster Reduction and Human Renovation Institution (DRI).
6. Dirección de Hidrografía y Navegación, Marina de Guerra del Perú.
7. Departamento de Oceanografía, CICESE.
*Co-authors of Okal and Dengler listed alphabetically.

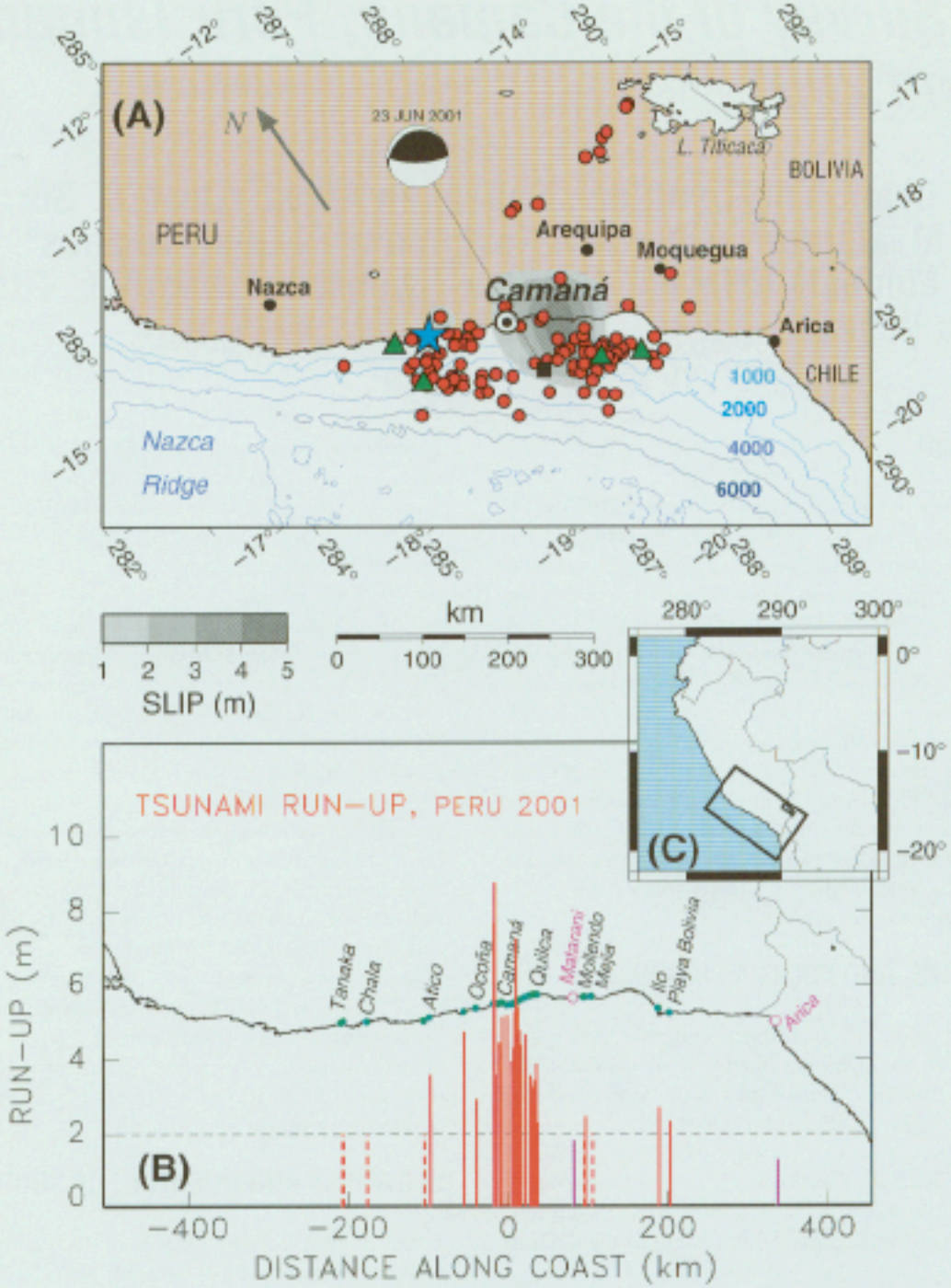


▲ **Figure 1.** (A) Map of the southern coast of Perú showing the epicenter of the mainshock (star) and of the one-month aftershocks (red dots); the larger events ($M > 5.8$) are shown as green triangles. The projection is an oblique Mercator, whose equator runs through Camaná at an azimuth of N125°E. The line of events running in the hinterland toward Lake Titicaca probably represents stress transfer into the Andes and should not be interpreted as defining the fault zone. Note the absence of aftershock activity just seaward of Camaná, suggesting intense strain release at that location during the mainshock. The areas shaded in gray show the results of Kikuchi and Yamanaka's (2001) tomographic investigation of the source slip (maximum 4.5 m). Also shown is the final Harvard CMT solution (rotated to conform to the orientation of the projection). The bathymetric contours are at 1,000, 2,000, 4,000 and 6,000 m and outline the Nazca Ridge at left. (B) Same projection as (A), showing the individual locations surveyed by the ITST along the coast (green dots), with the principal communities labeled. The purple open circles are the locations of the tide gauges at Matarani and Arica. The red bars show the amplitude of the individual runup measurements (see Table 1), plotted as a function of distance from Camaná along the equator of the oblique Mercator projection. Runup is measured relative to the −0.35 m tide at the time of the tsunami. The dashed line at 2 m is an estimate of the maximum high-water line, below which the tsunami was observed only as a drawdown (vertical dashed lines). Purple bars show the zero-to-peak amplitudes measured on the tide gauges. (C) Reference map showing the location of frames (A) and (B) (black box) within South America.

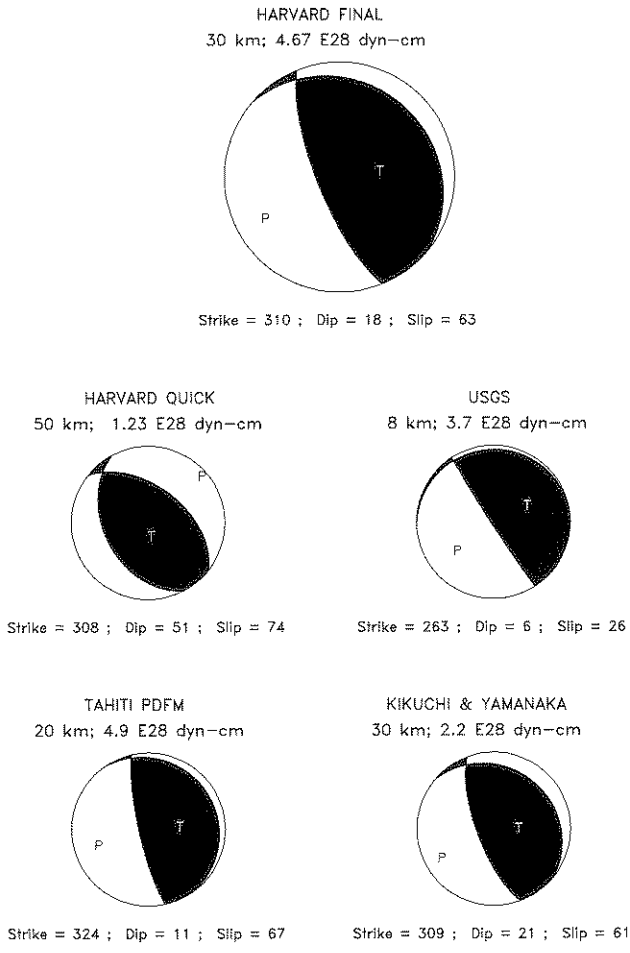


▲ **Figure 2.** Focal mechanism solutions proposed for the 2001 southern Perú earthquake. The top beach ball is the final Harvard solution, available from http://www.seismology.harvard.edu/CMTsearch.html. The other solutions were obtained in quasireal time by, respectively, the QUICK algorithm at Harvard, USGS (http://neic.usgs.gov/neis/FM/previous/0106.html), the Preliminary Determination of Focal Mechanism at Papeete, Tahiti (Reymond and Okal, 2000), and Kikuchi and Yamanaka (2001).

is further supported by an examination of *T* waves recorded on the IRIS broadband seismometer at Rarotonga (RAR; Figure 3). The ratio of *T*-phase energy flux to seismic moment is intermediate between those of the other two recent large Peruvian earthquakes, the tsunami earthquake at Chimbote on 21 February 1996 (M 7.4) and the regular Nazca event of 12 November 1996 (M 7.7). The 2001 Southern Perú earthquake shows a significant trend toward slowness without exhibiting the strong deficiency in high frequencies characteristic of a full-blown, truly slow "tsunami earthquake."

This observation is supported by the generally low macroseismic effects of the earthquake (Fierro and Wiss, 2001). Intensity levels reached only MMI VI in Camaná and along the coast, and MMI VII in the hinterland near Arequipa and Moquegua, where a lone strong-motion instrument recorded a peak acceleration of 0.3 g. The only structures destroyed by the earthquake in Camaná, 65 km away from the locus of strongest slip release, were poorly built adobe houses and shacks. The higher intensities in the hinterland probably express enhanced site response in the presence of weakly cemented clays and conglomerates (Keefer, 2001). Both this observation and the relative lack of major landsliding outside the Arequipa-Moquegua region contrast reports following other local earthquakes, including the much smaller event on 12 November 1996, which reached MM VIII at Nazca (Keefer, 2001).

## HISTORICAL BACKGROUND

The 2001 Perú earthquake and tsunami affected a 700-km stretch of the Peruvian coastline, extending from the Nazca Ridge to the Arica Bight at an azimuth of N125°E. The historical seismicity of this segment of the Nazca subduction zone was compiled by Dorbath *et al.* (1990), whose work is updated to 2001 in Figure 4. In 1604 and 1868 the region was the site of megathrust events that caused destruction of almost all structures over a 650-km-long area, with local tsunami runup reaching at least 15 m and Pacific-wide tsunami damage including in Japan. The 1604 and 1868 events are usually considered repeat earthquakes (Dorbath *et al.*, 1990; Swenson and Beck, 1996). During the interseismic window between them, significant (but not gigantic) earthquakes took place in 1687 and 1784. According to the reports compiled by Dorbath *et al.*, both of these shocks featured higher accelerations along the coast than those documented in 2001. The 1784 tsunami was probably smaller than that in 2001; there is no report of a tsunami for the earthquake of 21 October 1687 (not to be confused with a larger event that occurred farther north on the previous day and produced a tsunami that caused major damage to Callao). In this respect, and given its significantly slow character evidenced by little seismic destruction but a relatively damaging tsunami, the 2001 earthquake appears to have no directly comparable predecessor in the documented historical database. This illustrates the high variability in the patterns of earthquakes in a given subduction zone. Major earthquakes are not necessarily repetitive, as demonstrated for example by Ando (1975) in the Nankai Trough of Japan.

## THE TSUNAMI

The 23 June earthquake generated a destructive tsunami that reached the southern Peruvian coast within ten to thirty minutes and was observed at tide gauges throughout the Pacific. International media reported significant tsunami impact soon after the earthquake. Both Peruvian and international field investigation teams were organized to study the nature and extent of the tsunami in the impacted area.

### Post-tsunami Field Surveys

A reconnaissance team from the Peruvian Navy's Dirección de Hidrografía y Navegación conducted a survey of tsunami effects soon after the earthquake, noting evidence of inunda-

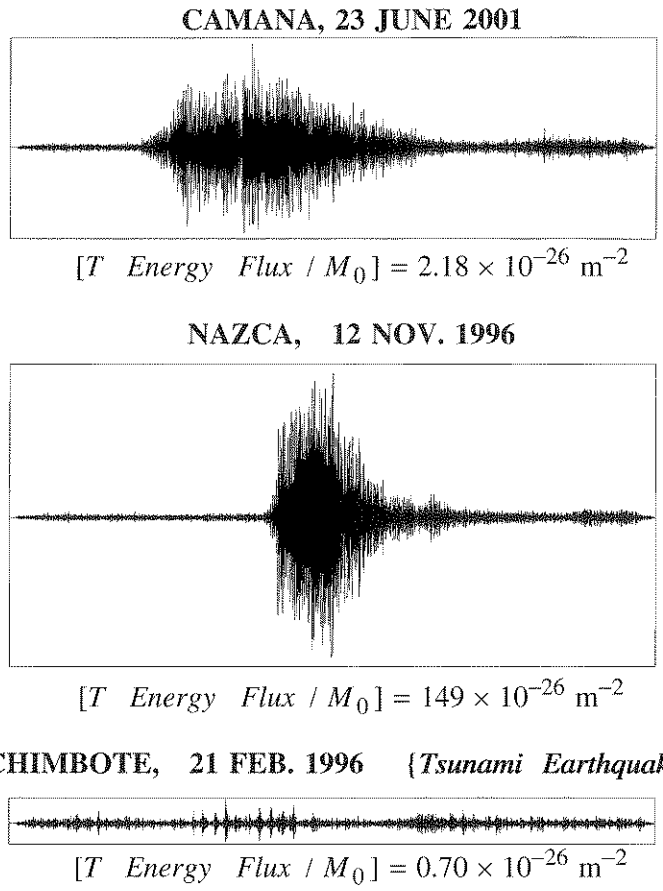


▲ **Figure 3.** Comparison of teleseismic *T*-wave records for three large Peruvian earthquakes. Top: the 2001 southern Perú earthquake; center: the 1996 Nazca earthquake; bottom: the 1996 Chimbote tsunami earthquake. All records are 1,000-second time windows from the broadband vertical (BHZ) channel at the IRIS station RAR (Rarotonga, Cook Islands) and are plotted on the same scale after applying a high-pass filter for $f > 2$ Hz. The *T*-phase energy flux to moment ratio is defined by Okal *et al.* (2002). Note its intermediate value for the 2001 wave train, the relatively long duration of the latter, and the strongly deficient *T* waves of the 1996 tsunami earthquake.

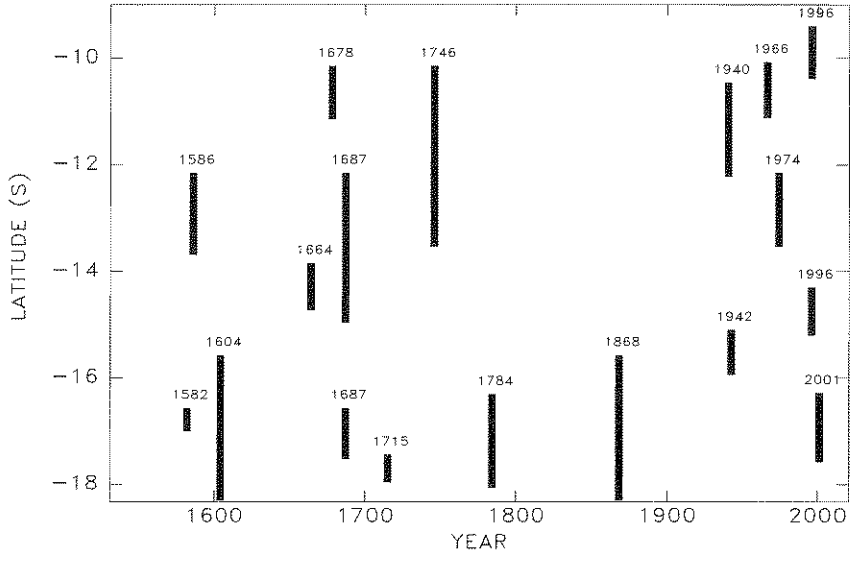


▲ **Figure 4.** Spatiotemporal distribution of rupture along the central and southern segments of the Peruvian subduction zone. This figure is adapted from Dorbath *et al.*'s (1990) Figure 8 and updated to 2001. The vertical bars indicate the extent of rupture involved in each of the major events. Note that because of the variable azimuth of the shoreline, the vertical axis, scaled in latitude, does not directly express rupture length.

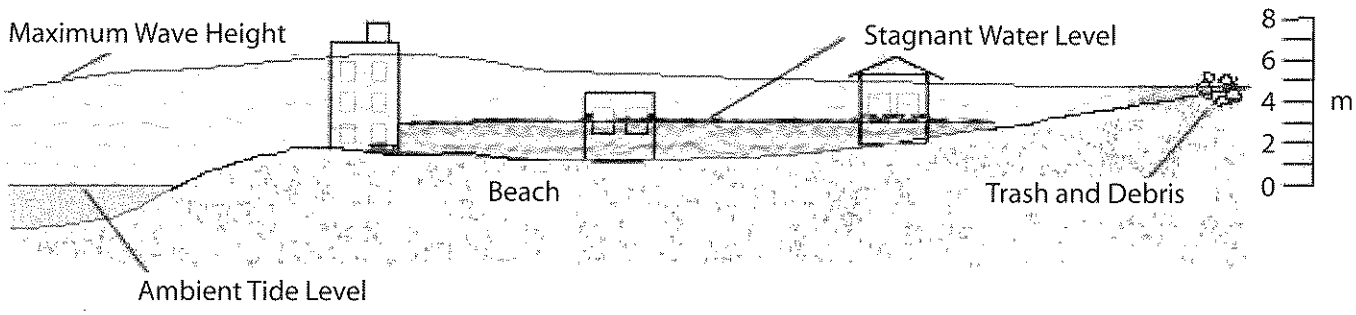


▲ **Figure 5.** Tsunami field data typical of the developed coastal area of Camaná. Inundation is the horizontal extent of water penetration; runup is the vertical elevation of the highest point on land flooded. High-water marks can sometimes be measured when sand and debris are deposited on the upper floors of buildings or in trees or power lines. In some cases water elevation can be estimated by height of damage such as blown-out windows or roofs. Buildings, walls, and trees may have one or more watermarks left by stagnant water.

tion from Atico to Ilo and major damage in the vicinity of Camaná. When significant impact was confirmed, an International Tsunami Survey Team (ITST) was organized to document the tsunami characteristics. The first ITST was in Perú from 6 to 15 July, measuring tsunami inundation and collecting eyewitness accounts along a 400-km stretch of coastline from Chala to Ilo. A second International Tsunami Survey Team visited Perú in September and focused on sediments deposited by the tsunami in the Camaná area. The second ITST also collected inundation data from a few sites that the first team was unable to reach. This report focuses on the characteristics of inundation and damage; a preliminary report on the sediment characteristics is posted at http://walrus.wr.usgs.gov/peru2/.

## Field Methods

The primary purpose of the first ITST was to document *inundation*, the horizontal extent of water penetration, and *runup*, the maximum vertical elevation of the land flooded, and to collect information on the tsunami effects. Evidence of inundation and runup is ephemeral and may disappear soon after the event. Teams use a combination of several methods:

1. Observing and recording water height and inundation indicators such as debris and strand lines; water marks on soil and buildings; elevation of damage such as broken windows and stripped roofs; debris and sands deposited on stairs, upper floors, and roofs (Figure 5). Care must be used in interpreting watermarks, as they relate to episodes when the water was still enough to leave a mark and are almost always less than the peak water height.
2. Interviewing eyewitnesses. It is easy to misinterpret debris and strand lines that may be caused by high tides and storm waves unless corroborated as a tsunami deposit by eyewitnesses. North of Ocoña and south of Quilca, observers reported that the positive tsunami waves did not extend as high as the high-tide mark. Without the witness observation, the tidal or storm berm could have been misinterpreted as the tsunami height. Human perception during catastrophic events can be skewed, however. There were several instances where an eyewitness reported wave heights that were incompatible with field evidence or other eyewitnesses. Many of the early media and NGO (nongovernmental organization) reports claimed water heights of 30 meters; the ITST found no credible watermarks over 8.8 meters. Whenever possible, ITST members spoke with several different groups of people to ensure a consistent story, and some interviews were recorded on videotape for permanent archiving at USC.
3. Surveying profiles. Lines were surveyed with optical or laser survey equipment along the beach profile from the breaking waves to the maximum inland extent of inundation. Elevations were calibrated relative to the ambient tidal level at the time of the tsunami.
4. Interviewing government officials and aid workers and collecting reports, maps, photographs, and other materials pertinent to the tsunami.

## Field Observations

Table 1 summarizes field survey data collected by the first ITST. Distance is measured along the coast relative to the Río Camaná delta at 16.64°S and 72.73°W, roughly the center of the inundation zone. At most sites estimates of both inundation and runup were obtained. The highest runup measured (8.8 m) was on the narrow beach at Playa Chira (see Figure 6A), where the coastal platform narrows to less than 500 meters and eyewitnesses described splashing of the waves against the cliffs. At several locations other indicators of high water were measured; the highest was a 7.2-m sand deposit and watermark on the third-floor stairs of the Titanic Club Playa Hotel (see Figure 7). The high-water values for the ports of Ilo and Arica are from tide gauges.

Table 1 also lists the setting of the locale where the data were obtained. The southern Peruvian coast is extremely arid and devoid of vegetation except in alluvial valleys fed by perennial streams and in developed and irrigated areas. Much of the coastline is steep and terminated by cliffs that drop abruptly to the water. Survey lines were restricted to the areas of coastal access. Most of the lines were located at fishing villages situated near coves and harbors (c), maize and onion

**TABLE 1**
**Tsunami Runup and Inundation Data**

| Location | Lat (°S) | Lon (°W) | Distance (km) | Setting[1] | Water Marks[2] (m) | Runup[3] (m) | Inundation (m) | Water Stopped by[4] |
|---|---|---|---|---|---|---|---|---|
| Tanaka | 15.71 | 74.50 | –215.5 | u | | bb | | w |
| Chala | 15.86 | 74.25 | –183.5 | c | | bb | | w |
| Punta Blanca | 16.23 | 73.70 | –112.6 | c | | bb | | w |
| Atico 1 | 16.23 | 73.61 | –104.7 | r | | 2.38 | 51.2 | w |
| Atico 2 | 16.23 | 73.61 | –104.0 | u | | 3.03 | 54 | w |
| Pescadores 1 | 16.44 | 73.24 | –58.7 | f | | 4.75 | 83.5 | |
| Pescadores 2 | 16.44 | 73.24 | –58.7 | l | | | 679.6 | |
| Ocoña | 16.45 | 73.10 | –44.8 | u | | 2.94 | 41.5 | p |
| Camaná 1 | 16.53 | 72.90 | –22.3 | u | | 7.71[s] | 254 | h |
| Camaná 2 | 16.53 | 72.90 | –21.7 | u | | 8.77[s] | 390 | h |
| Camaná 3 | 16.53 | 72.88 | –20.2 | u | 3.59 | 3.59 | 504 | p |
| Camaná 4 | 16.56 | 72.85 | –15.8 | f | | 4.46 | 725 | p |
| Camaná 5 | 16.57 | 72.82 | –12.4 | f | | 5.14 | 1000 | p |
| Camaná 6 | 16.62 | 72.78 | –6.1 | f | | 5.2 | 1358.5 | p |
| Camaná 7 | 16.64 | 72.74 | –1.3 | f | 3.95 | 2.78 | 1042.7 | p |
| Camaná 8 | 16.65 | 72.72 | 1.3 | f | 4.3–5.1 | 3.3 | 750 | p |
| Camaná 9 | 16.65 | 72.70 | 3.2 | f | 5.29 | 2.81 | 536.6 | p |
| Camaná 10 | 16.65 | 72.69 | 4.2 | f | | 4.89 | 785 | p |
| Camaná 11 | 16.65 | 72.69 | 5.1 | d | 7.25 | | | |
| Camaná 12 | 16.65 | 72.67 | 6.3 | d | | 3.79 | 483 | r |
| Camaná 13 | 16.66 | 72.65 | 8.8 | d | | 5.43 | 345 | r |
| Camaná 14 | 16.66 | 72.65 | 9.2 | d | 4.67 | 4.67 | 282 | h |
| Camaná 15 | 16.66 | 72.63 | 11.0 | d | | 4.78 | 240 | h |
| Camaná 16 | 16.66 | 72.61 | 13.0 | d | | 4.39 | 130 | h |
| La Bajada | 16.68 | 72.56 | 19.0 | u | | 4.67 | 160 | p |
| Pampa Grande | 16.69 | 72.50 | 25.3 | u | | 3.56 | 202 | p |
| Quilca 1 | 16.70 | 72.47 | 28.2 | u | | 3.25 | 110 | p |
| Quilca 2 | 16.70 | 72.46 | 30.0 | u | | 3.4 | 41.2 | p |
| Quilca 3 | 16.71 | 72.44 | 32.6 | c | | 3.18 | | |
| Quilca 4 | 16.71 | 72.43 | 32.7 | c | 2.62 | | | |
| Quilca 5 | 16.71 | 72.43 | 32.8 | c | 3.88 | 3.72 | 30 | |
| Quilca 6 | 16.72 | 72.42 | 33.9 | e | | 2.29 | 19.8 | |
| Puerto Matarani | 17.00 | 72.11 | 77.3 | c | 1.8[t] | | | |
| Matarani Beach | 17.03 | 72.01 | 87.9 | d | — | bb | | w |
| Mollendo North | 17.05 | 71.99 | 91.2 | d | — | bb | | w |
| Mollendo South | 17.05 | 71.97 | 92.7 | u | 2.45 | | 72.5 | w |
| Mejia | 17.09 | 71.91 | 100.9 | l | | bb | | w |
| Ilo | 17.63 | 71.34 | 183.6 | d | | 2.68 | 40 | w |
| Playa Bolivia Mar | 17.74 | 71.26 | 198.5 | u | | 2.33 | 72 | w |
| Arica, Chile | 18.47 | 70.33 | 326.4 | c | 1.3[t] | | | |

1. c: cove or harbor; d: developed coastal platform; f: agricultural field; l: lagoon; r: rocky beach; u: undeveloped coastal platform.
2. t: tide gauge reading.
3. s: watermark on cliff may represent splash; bb: below tidal berm.
4. h: cliff or hill; p: flat coastal platform; r: elevated road bed; w: wave slope.

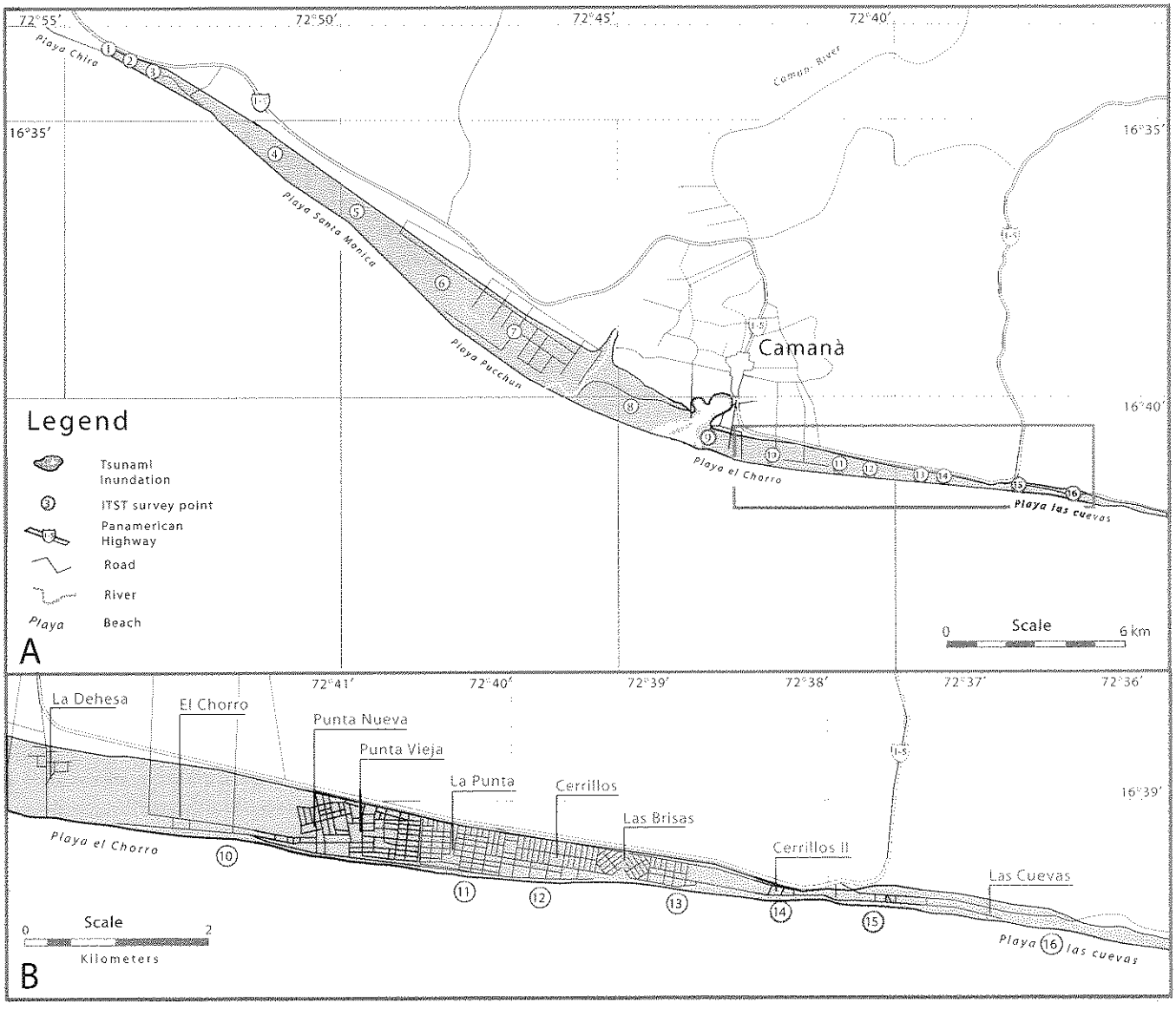


▲ **Figure 6.** Inundation map of the province of Camaná. (A) Coastline from Playa Chira to Las Cuevas. Numbers in circles refer to the Camaná survey lines given in Table 1. (B) The developed beach resort area. About 3,000 structures were within the inundation zone.

fields with extensive irrigation systems built on flat, low elevation coastal platforms near rivers (f), and resort communities developed along flat, wide beaches (d). Table 1 also notes the nature of where the water stopped: whether the waves ran up against an abrupt change in elevation such as a cliff (h) or road bed (r), dissipated on the relatively flat coastal platform (p), or never made it over the tidal berm (w).

Measured runups are shown in Figure 1B. The tsunami was observed by eyewitnesses along more than 400 km of coastline from Tanaka to Arica but produced wave heights well above high tide only from Atico to Quilca, and damaging waves along the 35 kilometers of coast straddling the Río Camaná. Figure 8A presents the distribution of runup heights, h, as a function of distance along the coastline. This data set features two main characteristics. First, the maximum value of water height is 7.25 m, excluding the higher values resulting from water splashing against the cliff at Playa Chira. This amplitude is approximately 1.5 times the maximum slip inferred from Kikuchi and Yamanaka's (2001) source tomography. This ratio is within the general range of systematic simulation experiments involving a wide variety of seismic sources obeying seismic scaling laws (Hoffman *et al.*, 2002).

Second, the runup data shown in Figure 8 are best fit by a function of the type

$$h = \frac{b}{\left(\frac{(x-c)}{a}\right)^2 + 1} \tag{1}$$

where $b$ is related to the maximum value of the height $h$ of runup, $a$ is related to its lateral spread with distance $x$ along


▲ **Figure 7.** Titanic Club Playa Hotel, La Punta. Sand and a water mark were observed on the third floor stairs at an elevation of 7.25 m above the sea level at the time of the tsunami. The windows were broken and the foundation was partially undermined, but this reinforced concrete building only 20 meters from the beach sustained little other structural damage.

the coast, and $c$ optimizes the position of the central peak. The optimal aspect ratio, $b/a = 4.2 \times 10^{-5}$, is adequately predicted by the simulation experiments of Hoffman *et al.* (2002). This value falls in the range of aspect ratios observed and computed in the near field for dislocation sources such as the 1992 Nicaragua earthquake (Figure 8B). This is in contrast to the much larger aspect ratios observed for the 1998 Papua New Guinea tsunami (Figure 8C), whose successful modeling requires an underwater landslide as its source (Synolakis *et al.*, 2002). Thus, the primary characteristics of the field of water heights surveyed after the 2001 Perú tsunami—absolute amplitude and lateral extent—are compatible with the seismologically derived dislocation source and do not require generation by an underwater landslide or slump. Preliminary modeling using a dislocation source appears to explain both far- and near-field tide gauge records of the tsunami adequately (Koshimura and Titov, 2001).

## TSUNAMI IMPACTS

The earthquake coincided with one of the lowest tides of the year, –0.35 meters below mean sea level (MSL). Outside of the province of Camaná, the tsunami had little direct impact. All eyewitnesses felt the earthquake strongly. They described a drawdown of the sea about 10 to 25 minutes after the earthquake. The water retreated to a distance 50 to 100 meters offshore, corresponding to an elevation of roughly 4 to 5 meters below the ambient water level. The water remained low for "a long time", variously described as 15, 20, or more minutes. In the fishing villages, residents were familiar with tsunami hazards and many expected a significant positive wave to follow, but the wave did not breach the high tide berm, at an elevation of about 2 meters above the sea at the time of the earthquake. Three or four more oscillations of the water were observed, but none of the waves reached any farther. No structures were reported damaged by the tsunami in these areas. An indirect impact was that local fishermen, fearful of another earthquake and a larger tsunami, were unwilling to take their boats to sea. There were also reports of coastal residents temporarily relocating to the highlands. Eyewitness descriptions of the tsunami north and south of Camaná are given in Borrero (2002).

Only one tide gauge was located within the area studied by the ITST. An analog United States Coast and Geodetic Survey flotation-type paper recorder is located at Puerto Matarani, about 125 km away from the epicenter and almost directly above the rupture zone. The record shows the onset of the tsunami as a small positive wave that begins about 6 minutes after the origin time of the earthquake, with the first peak (0.75 m) at 11 minutes. The second peak (1.86 m) at 38 minutes after the earthquake is the largest positive wave. A woman working in a souvenir shop 20 meters from the Matarani tide gauge house was the only eyewitness interviewed who noted the initial rise. She observed the boats in the harbor rise about one meter and then watched the water drain so that the boats rested on the sea floor. The port authorities then ordered an

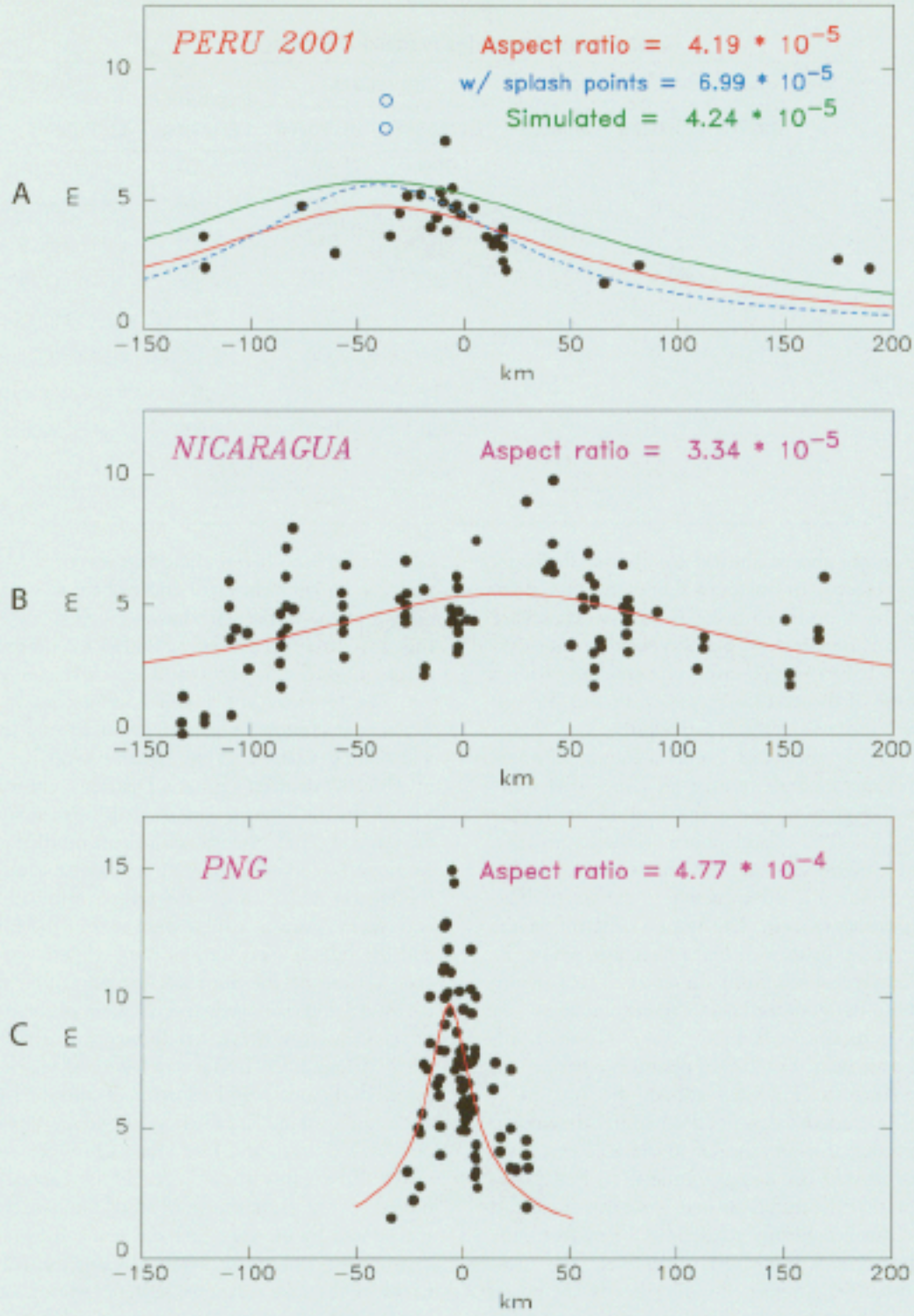


▲ **Figure 8.** Distribution of runup values as a function of distance along the beach, plotted for the 2001 Peruvian earthquake (A), the 1992 Nicaragua tsunami earthquake (B), and the 1998 Papua New Guinea (PNG) event (C). All three frames use common scales. The solid dots are the original runup values measured by the survey team for Perú, reported by Satake *et al.* (1993) for Nicaragua, and reported by Synolakis *et al.* (2002) for PNG. In each case, a function of the form (1), best fit by least-squares to the data set, is shown by the solid line and its aspect ratio *b*/*a* is printed. In the case of Perú, we delete from the data set the two large values of runup (open circles) corresponding to splashing against the cliff at Playa Chira; their inclusion would significantly bias the aspect ratio (dashed curve). The simulated curve (dash-dotted line) is predicted by a preliminary simulation using the crude model of a laterally uniform beach featuring a break of slope at 800 m. Note that the aspect ratio of the distribution of runup is similar to that of the Nicaraguan tsunami earthquake and remains one order of magnitude smaller than for the landslide-generated PNG tsunami.

**TABLE 2**
**Damages and Casualties in Camaná Province**

| District | Deaths | Missing | Injured | Structures | | Population Affected | Comments |
|---|---|---|---|---|---|---|---|
| | | | | Damaged | Destroyed | | |
| Camaná | 4 | 0 | 16 | 300 | 300 | 2,700 | deaths, injuries all tsunami |
| José Maria Quimper | 0 | 0 | 0 | 0 | 200 | 1,200 | out of inundation zones |
| Mariano Nicolás Valcárcel | 0 | 0 | 0 | 0 | 254 | 1,524 | out of inundation zones |
| Mariscal Cáceres | 3 | 2 | 0 | 30 | 115 | 780 | deaths, missing all tsunami |
| Nicolás de Piérola | 0 | 0 | 0 | 11 | 28 | 201 | out of inundation zones |
| Ocoña | 1 | 0 | 0 | 484 | 330 | 3,432 | mainly earthquake impacts |
| Quilca | 0 | 0 | 0 | 1 | 3 | 21 | mainly earthquake impacts |
| Samuel Pastor | 17 | 60 | 25 | 430 | 2,500 | 3,000 | deaths, injuries all tsunami |
| TOTAL | 25 | 62 | 41 | 1,256 | 3,730 | 12,858 | |

Source: INDEC (2001).

evacuation of the harbor area, so she did not observe the larger waves. Tide gauge records in northern Chile and at Callao, Perú also show an initial positive wave. The first tsunami wave along the southern Peruvian coast possibly was also positive, but because of its relatively small amplitude and the extreme low tide at the time of the earthquake, eyewitnesses did not notice the tsunami until the larger negative pulse.

The impact was significant in Camaná Province, where runups averaged 5 meters and inundation penetrated more than 1 km inland. Figure 6 shows the inundation in the Camaná area based on ITST survey points (circled numbers), photographs, and eyewitness accounts. The tsunami reached at least 500 meters inland in all areas where the waves dissipated on the flat coastal platform. The deepest penetration was over the flat agricultural fields near Playa Pucchún, where the water extended nearly 1.4 km from the coast. The tsunami also flooded the boundaries of the lagoon and extended at least 1 km up the Río Camaná (Ocola, pers. comm.). To the north and south of the river delta, the coastal platform narrows and cliffs and the Pan American Highway stopped the tsunami.

Eyewitnesses in Camaná described an initial drawdown that lasted 15 minutes or more, similar to the accounts from the communities outside the damage zone described previously. Most agreed that the initial positive wave was small and did not overtop the beachfront road only 15 m from the water's edge. The second and third waves were the most destructive and of similar impact, flooding nearly the entire inundation zone. Eyewitnesses described fast, turbulent flows as the water withdrew. Many survivors self-evacuated upon observing the initial withdrawal of the sea or after being urged by others to evacuate; no one responded to the ground shaking even though all felt the earthquake strongly. There were several reports of people going out to look at the exposed sea platform when the water withdrew. The situation was different for farm workers. The workday ends at 4:00 PM on Saturdays, and even when told by others to evacuate, some were reluctant to leave before their shift was over. Many of the fields were too far from the coast and/or behind a berm or irrigation dike, and the initial withdrawal could not be seen. Much of the area remained partially flooded for several days after the tsunami, restricting access and search/rescue operations.

The province of Camaná (population 53,000) has eight districts that include coastal resort towns, farming regions, and fishing villages. Table 2 summarizes the damage in the province by district. Camaná District includes the city center (out of the inundation zone), the mixed resort/farming area of El Chorro, and the farming community of La Dehesa. Mariscal Cáceres District extends along the coast west from the lagoon and includes the farm communities of Pucchún and Santa Monica, which were within the inundation zone, and the inland areas west of the Camaná City center, which was outside of the zone of flooding. The majority of the destroyed and damaged structures, all of the deaths, and most of the injuries in these two districts are attributed to the tsunami. About 2,500 hectares of farmland was flooded, destroying all of the onion and maize crops and the irrigation control and canal system. The districts of Nicolás de Piérola, Mariano Nicolás Valcárcel, and José Maria Quimper are located to the north and northwest of Camaná City center and are entirely outside of the tsunami zone; all of the damage in these areas was caused by the earthquake. Ocoña, a farming and fishing town about 50 km northwest of Camaná and the city closest to the earthquake epicenter, suffered some damage to the harbor from the tsunami, but the one death here and most of the structural damage are attributed to the earthquake. The impact in Quilca, the small fishing village 30 km east of Camaná, was minor and caused by the ground shaking.

The district of Samuel Pastor was hardest hit. It includes the resort communities of Punta Nueva, Punta Vieja, La Punta, Cerrillos, Las Brisas, Cerrillos II, and Las Cuevas and the farmlands just west of Punta Nueva. The developed part of the district lies almost entirely within the tsunami inundation

zone. The 87 dead and missing, all of the injuries, and all destroyed structures are attributed to the tsunami. Officials estimated that only about 15 of the 3,000 structures within the inundation zone survived the tsunami with no structural damage. Fortunately these resort towns were almost uninhabited at the time of the earthquake. Most of the hotels, restaurants, and discotheques were closed, and only a few summer home caretaker families were in residence. During the summer months from December to March, more than 5,000 people live in the area and hundreds of tourists occupy the beach hotels.

Of the documented tsunami deaths, eight were children and sixteen adults (INDEC, 2001). No demographic information was available for the missing. Fifty-five percent of the tsunami victims were male, in contrast to the victims in the other provinces killed by ground shaking effects, of which 65% were female. Of the adults, half were aged between 30 and 50 and none was over 70. Of the shaking-related deaths in Moquegua, Arequipa, and the other inland areas, 40% were over 70 and fewer than 30% of adults were in their prime. A likely cause of the difference is that most of the tsunami victims were adult field workers and house sitters, whereas in the inland areas the elderly and the very young were more likely to be indoors on a Saturday afternoon and were crushed when houses collapsed. Only about 40 people were injured by the tsunami, less than half the number killed or missing. This is typical of tsunamis where people caught in the water are more likely to be killed than injured. In the 1998 Papua New Guinea tsunami, more than 2,100 people were killed and fewer than 1,000 injured (Dengler and Preuss, 2002). In contrast, ground shaking is much more likely to injure than kill. In the areas outside the inundation zone, 51 people died and more than 2,700 were reported injured from the Perú earthquake (INDEC, 2001).

Damage to structures in the inundation zone was nearly total. Buildings in the coastal area are of three general types. In the farming areas and fishing villages, weak adobe structures and shacks of bamboo and other lightweight materials predominate. In the resort area, the majority of structures were less than ten years old and substantial. Most were built on concrete slab foundations about 25–30 cm thick with reinforced columns at the corners. Preformed brick blocks were filled in between the columns to make the walls. A number of hotels, some restaurants, and a few homes were built of reinforced concrete with thicker foundations. No wood structures were in the inundation zone. Eyewitnesses reported that the vibrations caused damage to some of the shacks and adobe structures and caused a few to collapse, but none of the stronger buildings was affected by the ground shaking.

The weak adobe structures and bamboo shacks were obliterated by the tsunami and no sign of them remained afterward. The infilled wall structures also performed poorly; walls perpendicular to the incoming wave direction were typically blown out (Figure 9). Scour was common at the corners of structures, undermining the thinner slab foundations (Figure 10). Scour also was concentrated along the edges of roads and near earthen berms separating fields. In contrast, there was no evidence of scour on the smooth undeveloped coastal platform along Playa Chira. Reinforced concrete structures with thicker foundations were most likely to survive, even when located close to the beach (Figure 7). The degree of structural damage did not correlate with distance from the coast; buildings near the limit of inundation were as likely to be destroyed as those closest to the beach. The beachfront structures were mainly restaurants, hotels, and discotheques and appeared to be more substantially constructed than the summer homes farther back from the coast.

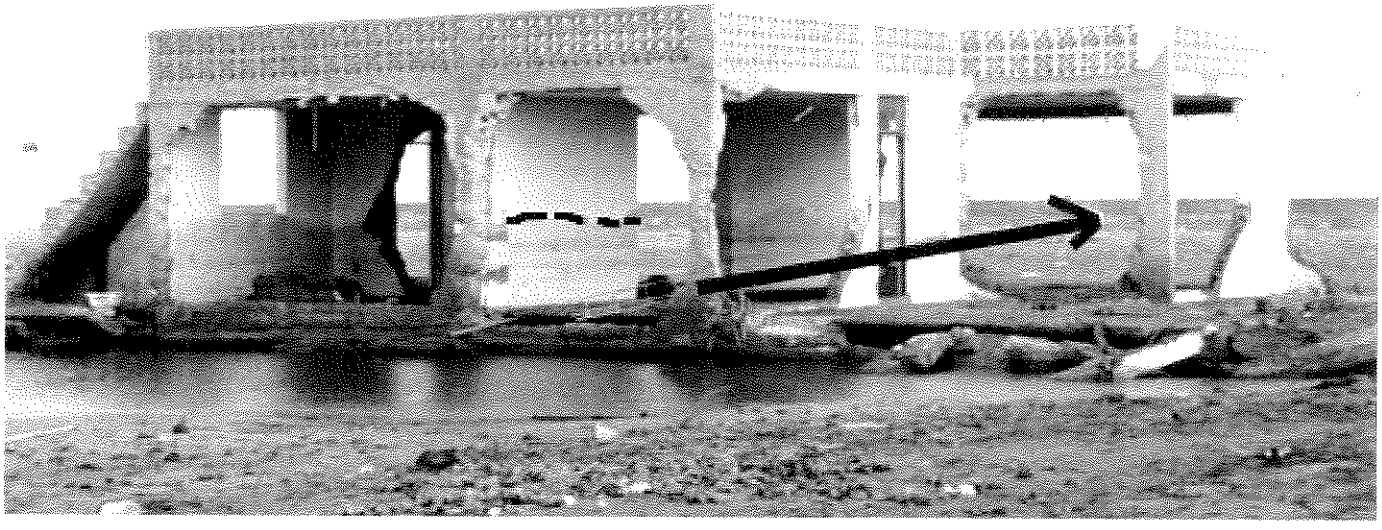

▲ **Figure 9.** Damaged summer home, La Punta. Typical construction consists of reinforced columns on a 20–30-cm-thick concrete slab foundation with unreinforced brick-infilled walls. Walls perpendicular to the direction of the tsunami (black arrow) failed. Dashed line shows a stagnant water mark.

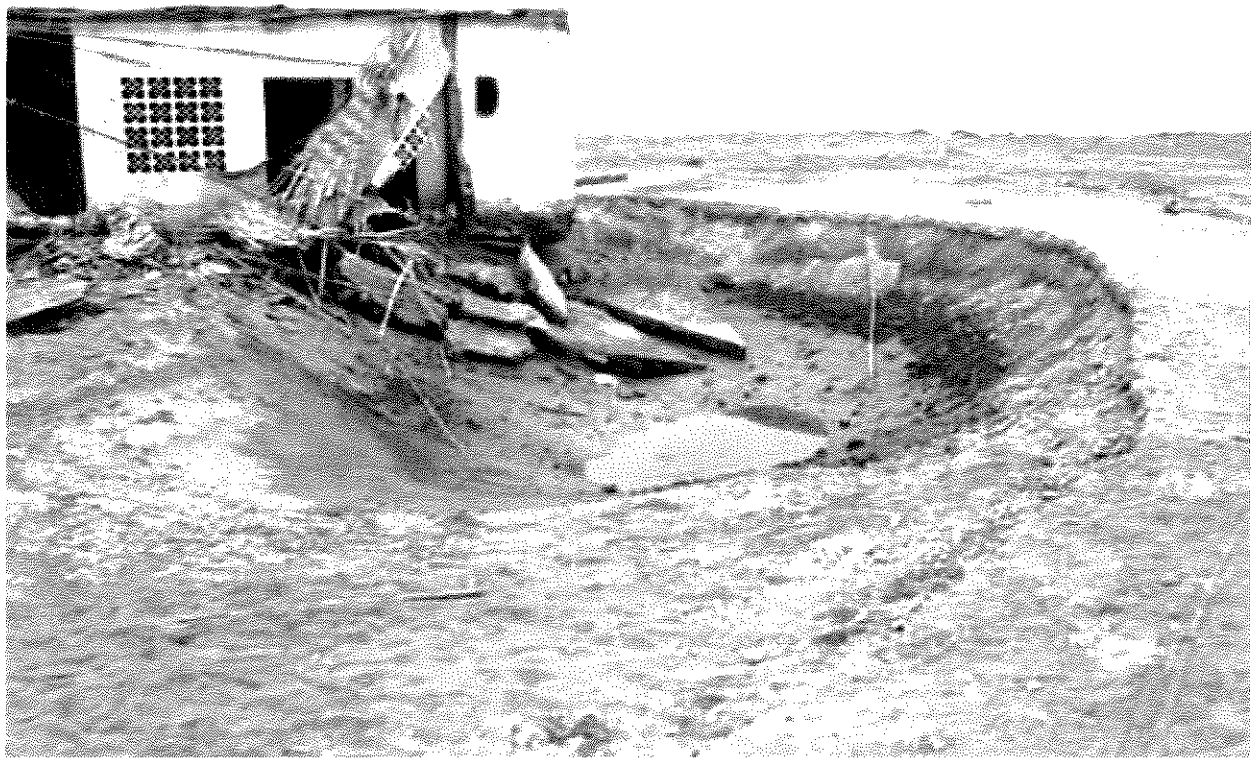

▲ **Figure 10.** Scour around the southwest corner of a La Punta house. Scour was observed at the corners of almost every structure in the inundation zone and next to paved roads.

## DISCUSSION

The 23 June earthquake generated a tsunami that produced waves large enough to cause significant damage along 35 km of coast and to be observed by eyewitnesses for more than 400 km. It was the most widely recorded tsunami in the Pacific since the one caused by the 1994 ($M_w$ 8.2) Kuril Islands earthquake. The size of the 23 June tsunami appears to be consistent with a seismogenic source; the largest waves averaged 5 meters, with some approaching 7 to 8 meters, similar in scale to the maximum slip on the fault. The aspect ratio of the runup height to distance along the coast does not reach the high values characteristic of a landslide source. The seismic characteristics ($\Theta$, $T$ phase, intensity) of the earthquake all suggest a tendency toward slowness, but not values characteristic of a true "tsunami" earthquake.

While the amplitude of the tsunami scaled consistently with the size of its source, it was somewhat surprising that, outside of the municipality of Camaná, the size of the positive waves may have been significantly less than the drawdown. The eyewitness accounts both north and south of Camaná consistently described a withdrawal of the water with a vertical amplitude on the order of 5 meters. Many expected the positive wave to be equally large, evacuated to high ground, and were surprised that the waves did not overtop the high tide line. The tide gauge recordings at Matarani and Arica, Chile, the two closest stations, do not exhibit any profound asymmetry but are both located in harbors, and the waves are affected by local resonances. The asymmetry, if real, might also result from a combination of the complex distribution of slip on the fault and permanent uplift of the coast. Kikuchi and Yamanaka's (2001) slip model (Figure 1A) implies a large uplift near the coast about 65 km east-southeast of Camaná that could explain an initial drawdown as the water flowed away from the uplifted area toward offshore. The same slip model suggests 0.5 to 1 m of coseismic uplift of the coast between Quilca and Chala, possibly making the positive wave appear smaller in much of the area. It is also possible that the extreme low tide may have biased the eyewitness observations.

The tsunami caused major damage to the province of Camaná and was far more damaging than ground shaking in this area. The largest waves produced by the June 2001 earthquake unfortunately occurred with the most developed beach area along the southern Peruvian coast. Tsunami waves penetrated more than 1 km inland and damaged or destroyed nearly all of the 3,000 structures in this zone. Damaged structures were built on ground below 5 meters in elevation above sea level, reaffirming the hazards of development along exposed coastal platforms at low elevation. Poorly built adobe buildings were obliterated and almost all brick-infilled-wall structures destroyed. The few structures that survived had more reinforcement and thicker foundations.

While the extent of inundation and the number of structures damaged or destroyed was significant, the number of lives lost was much less than caused by other recent tsunamis.

It was also lower than what might have been expected from the scale of structural damage within the inundation zone. Several reasons exist for the relatively light loss of life:

1. Time of year. First and foremost, the earthquake and tsunami occurred in winter. The summer resident population of the Camaná beach towns increases by 5,000 people plus an additional influx of tourists. Had the same earthquake occurred in the summer when the beach discotheques, hotels, and cafés were full, casualties would undoubtedly have been much higher.
2. Time of day. The earthquake and tsunami occurred during daylight hours. Seeing the water retreat was the key to self-evacuation. Had the earthquake occurred at night, it is likely that fewer people would have responded.
3. Ambient sea level. The tsunami coincided with a –35 cm tide, one of the lowest tides of the year. A high tide would have added more than 1 meter to the final runup. The seas were also relatively quiet the day of the earthquake. Large winter storm swells would have further exacerbated the impact.
4. Initial drawdown of water and period of wave. As discussed above, it is not clear whether the large drawdown was preceded by a positive wave, in which case the latter was of low amplitude. For the purpose of this discussion, a key aspect of the tsunami strongly mitigating its impact was that the first *noticeable* motion of water was a *large retreat.* This and the significantly long period of the phenomenon (at least 15 minutes) allowed even people unfamiliar with tsunamis to react to the very unusual state of the sea and to seek higher ground.
5. A tsunami-aware coastal population. Many of the people interviewed knew what tsunamis were, recognized the water drawdown as a sign of danger, and self-evacuated. This was true primarily among the traditional coastal communities of fishermen, who "know the sea", are educated about tsunami hazards, and had in many cases experienced or heard about similar events in the past. By contrast, the victims were farm workers and domestic house sitters hired for the winter, many of whom came from inland and were unaware of tsunami hazards.
6. Relatively low exposure. The 300-km-long coastline adjacent to the rupture is mostly steep and arid. Only along the river deltas does it constitute habitable land at low elevation. Consequently, both the area available for flooding and more importantly the population at risk were minimized.

We note that the survivors generally used the drawdown of the water, rather than the earlier ground shaking during the earthquake, as the trigger to self-evacuation. This behavior among a well informed community at first surprised some of the ITST members, since in principle the ground shaking would have given them an additional 10 to 15 minutes' head start. It must be borne in mind that the real-time human evaluation of tsunami hazard based on shaking is next to impossible; even a seasoned observer would do no better than estimate intensity, which is a notoriously poor proxy for static moment. Strongly felt earthquakes are common along the southern Peruvian coast, and very few produce damaging tsunamis. Perhaps for this reason the ancestral wisdom passed down from previous generations is that "when the water goes down the sea comes back big", and the fishing communities have adopted the retreat of the sea as a traditional, and arguably rational, warning permitting a reduction in false alarms. But the next major tsunami to hit the Peruvian coast might not begin with a substantial drawdown, or it may happen during the night when the sea cannot be readily observed. Therefore, tsunami hazard education programs need to encourage response to shaking, even if it results in unnecessary evacuations.

The 2001 tsunami does not represent the worst-case scenario for the inhabitants of the southern Peruvian coast. The 1604 and 1868 events certainly produced waves that were twice as high and impacted a much larger part of the coast. Even the relatively distant 1877 Chilean earthquake produced tsunami waves of larger amplitude than in 2001 at many locations along the southern coast of Perú (Solov'ev and Go, 1984). While the 2001 earthquake may have relieved part of the accumulated strain along the interface boundary, a recurrence of a larger event is still possible and poses a significant risk. Education about the local tsunami hazard is both the most economical and most effective way to reduce fatalities from future events. ■

## ACKNOWLEDGMENTS

First and foremost, we thank the people of Perú for their willingness to talk to us and assist our field efforts during a time of extreme emotional and physical duress. The effort of the International Tsunami Survey Team was supported by the National Science Foundation under Grant Number 01-29999. Additional funding was provided by Northwestern University, Humboldt State University, and Pacific Gas and Electric Company, with additional support from the Peruvian Navy, Federal Emergency Management Agency, National Tsunami Hazard Mitigation Program, JISAO of the University of Washington, USDA Forest Service, NOAA/PMEL, and the U.S. Geological Survey. We thank Professor Leonidas Ocola of the Instituto Geofísico del Perú for providing additional information on the inundation zone in Camaná and on the intensity of ground shaking. We thank Dominique Reymond of the Laboratoire de Géophysique, Papeete, for the PDFM solution. We thank Admiral Hector Soldi, Director of the Hydrographic Office of the Peruvian Navy, for his support, as well as Captain Mauro Cacho for logistical help. Discussions with Edmundo Norabuena and Costas Synolakis are also acknowledged. Thanks to Bob Peters, Guy Gelfenbaum, and Bruce Jaffe of the second ITST team for additional survey data. Irina Hoffman helped with the early simulations shown in Figure 8. Figure 1 was prepared using the *GMT* software (Wessel and Smith, 1991). A special thanks to Henry Oviedo, who has continued to communicate information on Camaná impacts and recovery to the ITST team.

## REFERENCES


Ando, M. (1975). Source mechanisms and tectonic significance of historical earthquakes along the Nankai Trough, Japan, *Tectonophysics* **27**, 119–140.

Borrero, J. for the ITST (2002). Field survey of the June 23, 2001 earthquake and tsunami in southern Peru, ASCE Solutions to Coastal Disasters, in Lesley Ewing and Louise Wallendorf (editors), *Solutions to Coastal Disasters '02,* February 24–27, 2002, San Diego, CA, 892–904.

Dengler, L. and J. Preuss (2002). Mitigation lessons from the Papua New Guinea tsunami of 17 July 1998, *Pure and Applied Geophysics* (in press).

Dorbath, L., A. Cisternas, and C. Dorbath (1990). Assessment of the size of large and great historical earthquakes in Peru, *Bulletin of the Seismological Society of America* **80**, 551–576.

Fierro, E. and J. Wiss (2001). Structural damage, in Preliminary observations on the Southern Peru earthquake of June 23, 2001, EERI Special Earthquake Report—November 2001, *Earthquake Engineering Research Institute Newsletter* **35**, 7–8.

Fukao, Y. (1979). Tsunami earthquakes and the subduction process near deep-sea trenches, *Journal of Geophysical Research* **84**, 2,303–2,314.

Hoffman, I., E. A. Okal, and C. E. Synolakis (2002). Systematics of the distribution of tsunami runup along coastlines in the near-field for dislocation sources with variable parameters (abstract), *Eos, Transactions of the American Geophysical Union* **83**, WP54.

INDEC (2001). Resumen final de daños en distritos afectados por el sismo del 23-06-01 y sub-siguientes ocurridos en el sur del pais, Instituto Nacional de Defensa Civil, Lima, Peru, http://www.indeci.gob.pe/resumdist27nov08h.htm.

Kanamori, H. (1972). The mechanism of tsunami earthquakes, *Physics of the Earth and Planetary Interiors* **6**, 349–359.

Keefer, D. K. (2001). Landslides (abstract), in Preliminary observations on the Southern Peru earthquake of June 23, 2001, EERI Special Earthquake Report—November 2001, *Earthquake Engineering Research Institute Newsletter* **35**, 4–5.

Kikuchi, M. and Y. Yamanaka (2001). EIC Seismological Note Number 105, http://wwweic.eri.u-tokyo.ac.jp/EIC/EIC_news/105E.html.

Koshimura, S. and V. Titov (2001). Preliminary model results for the 23 June 2001 Peruvian tsunami, Proceedings of the International Tsunami Symposium 2001 (ITS 2001) (on CD-ROM), Pacific Marine Environmental Laboratory, NOAA, Session 2, No. 2-2, 379.

Newman, A. V. and E. A. Okal (1998). Teleseismic estimates of radiated seismic energy: The $E/M_0$ discriminant for tsunami earthquakes, *Journal of Geophysical Research* **103**, 26,885–26,898.

Okal, E. A., P.-J. Alasset, O. Hyvernaud, and F. Schindelé (2002). The deficient *T* waves of tsunami earthquakes, *Geophysical Journal International* (in press).

Okal, E. A. and J. Talandier (1989). $M_m$: A variable period mantle magnitude, *Journal of Geophysical Research* **94**, 4,169–4,193.

Polet, J. and H. Kanamori (2000). Shallow subduction zone earthquakes and their tsunamigenic potential, *Geophysical Journal International* **142**, 684–702.

Reymond, D. and E. A. Okal (2000). Preliminary determination of focal mechanisms from the inversion of spectral amplitudes of mantle waves, *Physics of the Earth and Planetary Interiors* **121**, 249–271.

Satake, K., J. Bourgeois, K. Abe, Y. Tsuji, F. Imamura, Y. Iio, H. Katao, E. Noguera, and F. Estrada (1993). Tsunami field survey of the 1992 Nicaragua earthquake, *Eos, Transactions of the American Geophysical Union* **74**, 146, 156–157.

Solov'ev, S. L. and Ch. N. Go (1984). Catalogue of tsunamis on the eastern shore of the Pacific Ocean, *Canadian Translation of Fisheries and Aquatic Sciences*, Ottawa, No. 5078, 285 pp.

Swenson, J. L. and S. L. Beck (1996). Historical 1942 Ecuador and 1942 Peru subduction earthquakes, and earthquake cycles along the Colombia-Ecuador and Peru subduction segments, *Pure and Applied Geophysics* **146**, 67–101.

Synolakis, C. E., J.-P. Bardet, J. C. Borrero, H. L. Davies, E. A. Okal, E. A. Silver, S. Sweet, and D. R. Tappin (2002). The slump origin of the 1998 Papua New Guinea tsunami, *Proceedings of the Royal Society* (London), Ser. A, **458**, 763–789.

USAID (2001). Peru Earthquake Fact Sheet #6 (FY 2001), U.S. Agency for International Development, ReliefWeb http://www.reliefweb/int.

Wessel, P. and W. H. F. Smith (1991). Free software helps map and display data, *Eos, Transactions of the American Geophysical Union* **B72**, 441, 445–446.



*Department of Geological Sciences*
*Northwestern University*
*Evanston, IL 60201, USA*
**emile@earth.nwu.edu**
*(E.A.O., B.M.G.)*

*Department of Geology*
*Humboldt State University*
*Arcata, CA 95521, USA*
*(L.D., S.A.)*

*Department of Civil Engineering*
*University of Southern California*
*Los Angeles, CA 90089, USA*
*(J.C.B., M.S.)*

*Pacific Marine Environmental Laboratories*
*NOAA*
*7600 NE Sand Point Way*
*Seattle, WA 98115, USA*
*(S.K., V.V.T.)*

*Disaster Reduction and Human Renovation Institution (DRI)*
*1-5-2 Wakihama Kaigan-Dori*
*Chuo-Ku, Kobe 651-0073*
*Japan*
*(S.K.)*

*Dirección de Hidrografía y Navegación*
*Marina de Guerra del Perú*
*Avda. Gamarra 500*
*El Callao, Perú*
*(G.L., D.O., F.V.)*

*Departamento de Oceanografía*
*CICESE*
*Ensenada, B.C.*
*México*
*(M.O.F.)*